

COMPRESSIVE CLASSIFICATION FOR THROUGH-THE-WALL RADAR IMAGING

Mark R. Balthasar, Michael Leigsnering, Abdelhak M. Zoubir

Signal Processing Group
Technische Universität Darmstadt
Darmstadt, Germany

ABSTRACT

Through-the-Wall Radar Imaging (TWRI) is an emerging technology, desirable for a variety of military and civilian applications. Some of these applications require the ability to make a rapid decision on the contents of a target scene, rather than reconstruct it perfectly. In this work, we address this problem by modifying the smashed filter proposed by Davenport et al., which is based on compressive sensing (CS) theory. We introduce two compressive classification methods, which allow for an efficient hardware implementation as well as deliver accurate classification results in the considered scenarios using only a fraction of the available data.

Index Terms— Through-the-Wall, radar imaging, compressive sensing, compressive classification

1. INTRODUCTION

Through-the-Wall Radar Imaging (TWRI) is a very promising field of research with a variety of applications including military, police, and fire brigade missions as well as search and rescue in the aftermath of natural disasters [1, 2]. By delivering information about obscured areas, which cannot be observed by other means, it provides a way to estimate the layout of an observed scene as well as localize, identify, and classify possible obscured targets.

Conventional TWRI systems usually form an image from the gathered data and apply target detection before classifying on the obtained features [3, 4]. Compressive sensing (CS) has been shown to tremendously decrease the amount of necessary data for high-resolution TWRI reconstruction [5]. Aspects in sparse reconstruction of extended targets have been studied in [6], however, it is unclear if these images can be used for classification as the image statistics differ strongly from beamformed images. Apart from that, there are many applications, such as search and rescue missions, in which it is crucial to rapidly decide on the scene under observation rather than reconstruct its layout perfectly. This work seeks to provide a solution to this problem by bringing CS theory to the classification domain. Our aim is to achieve reliable classification using only a small amount of measurements, for

which no imaging would be possible. To this end, we will resort to the smashed filter, which was developed by Davenport et al. in [7]. This algorithm offers a way to apply compressive classification (CC) in image target classification by using a maximum likelihood classifier (MLC) directly on compressed measurements. It is even able to deal with arbitrary perturbations, such as a shift or rotation, by prepending a maximum likelihood estimator (MLE).

We propose two adaptations of the smashed filter for the application in TWRI, namely Fixed Frequency Classification (FFC) and Fixed Antenna Element Classification (FAEC), which randomly combine measurements in the space or frequency domain, respectively, before applying the smashed filter. Both methods can be efficiently implemented and deliver close to perfect classification in the considered scenarios using less than 0.1 % of the available data.

In Sections 2 and 3, we will briefly revisit the smashed filter and introduce the TWRI signal model used in our experiments, respectively. In Section 4 FFC and FAEC are presented. Section 5 compares their performance to a standard method in a simulated as well as a real TWRI scenario.

2. THE SMASHED FILTER

The smashed filter is a two-step algorithm, consisting of a MLE, i.e. a least-squares estimator (LSE) in the case of additive white Gaussian noise (AGWN), followed by a MLC. It was initially developed to classify compressed images of objects that are taken using a single-pixel camera, a detailed description of which can be found in [8].

Compressive measurements of a signal $\mathbf{x} \in \mathbb{R}^N$ in a noisy image can mathematically be expressed as

$$\mathbf{y} = \Phi(\mathbf{x} + \mathbf{w}), \quad (1)$$

where $\Phi \in \mathbb{R}^{M \times N}$, $M \leq N$ is a pseudorandom orthoprojector and \mathbf{w} denotes AWGN with variance σ^2 [7]. Note, that Φ can either be filled with zeros and ones, which corresponds directly to the single-pixel camera imaging process, or with ± 1 .

For each class C_i , $i = 1, \dots, P$, containing the signal \mathbf{s}_i , the smashed filter requires access to a set of training data,

i.e. a manifold M_i , containing all possible transformations $\mathbf{x} = f_i(\boldsymbol{\theta}, \mathbf{s}_i)$ of the signal, parametrized by $\boldsymbol{\theta}$. Note that the function f_i could represent scaling, rotation, or translation of the object or the whole scene in an imaging scenario. If f_i is unknown, we can resort to a data-based representation using training data.

The smashed filter [7] first estimates the closest point on each manifold M_i to the observed signal \mathbf{y} using a LSE, which is equal to finding the most probable transformation for each class. Mathematically, this is given by

$$\hat{\boldsymbol{\theta}}_i = \arg \min_{\boldsymbol{\theta} \in \Theta_i} \|\mathbf{y} - \Phi f_i(\boldsymbol{\theta}, \mathbf{s}_i)\|_2^2. \quad (2)$$

In the second step, MLC selects the manifold and thereby the class for which the distance between \mathbf{y} and the closest point on the manifold is minimal, as

$$C(\mathbf{y}) = \arg \max_{i=1, \dots, P} p(\mathbf{y} | \hat{\boldsymbol{\theta}}_i, C_i), \quad (3)$$

where the likelihood $p(\mathbf{y} | \hat{\boldsymbol{\theta}}_i, C_i)$ is approximated by

$$p(\mathbf{y} | \hat{\boldsymbol{\theta}}_i, C_i) = \frac{1}{(2\pi\sigma)^{M/2}} e^{-\frac{1}{2\sigma} \|\mathbf{y} - \Phi f_i(\hat{\boldsymbol{\theta}}_i, \mathbf{s}_i)\|_2^2}. \quad (4)$$

Note that this expression holds exactly, if Φ is an orthoprojector [7].

3. THROUGH-THE-WALL RADAR IMAGING SIGNAL MODEL

Consider a monostatic uniform linear array of A antenna elements t_a placed at a distance z_{off} from the observed target area. The stepped-frequency approach is used to synthesize an ultrawideband (UWB) pulse. This is done by transmitting short continuous wave segments at U different frequencies f_u for each antenna element, exploiting the Fourier equivalency in the process [1].

In the frequency domain, the received signal at array element t_a and frequency f_u can be regarded as a superposition of P point targets [1]:

$$r[u, a] = \sum_{p=0}^{P-1} \sigma_p e^{-j2\pi f_u \tau_{pa}}, \quad (5)$$

where σ_p denotes the target reflectivity of target p and τ_{pa} is the two-way propagation delay between target p and antenna element t_a . If a wall is present, the EM waves are refracted according to Snell's law and τ_{pa} has to be calculated accordingly. In the absence of a wall, however, τ_{pa} can simply be computed using the Euclidean distance d_{pa} between target p and antenna element a :

$$\tau_{pa} = \frac{2 \cdot d_{pa}}{c_0} \quad (6)$$

where c_0 denotes the speed of light.

Eventually, we obtain an $U \times A$ measurement matrix, representing the target area in the frequency-space domain. Conventional imaging and classification algorithms would apply beamforming, for example, employing Direct Frequency Domain Image Formation [9]. Since we are not interested in the exact layout of the target scene and, thus, want to skip the imaging step, the smashed filter shall be applied directly to the $N = U \times A$ measurements. As these do not correspond to actual pixel locations, the algorithm has to be adapted in order to work in a TWRI scenario. In the following, we will explore two such adaptations.

4. COMPRESSIVE CLASSIFICATION FOR THROUGH-THE-WALL RADAR IMAGING

As mentioned earlier, many TWRI applications require rapid classification decisions on the scene under observation. Due to portability reasons, it is, furthermore, desirable to make reliable decisions with as few measurements as possible. FFC and FAEC are two approaches at bringing the smashed filter to the classification domain. By linearly combining random measurements in the space and frequency domain, respectively, they form compressive measurement vectors to which the smashed filter is applied.

4.1. Fixed Frequency Classification

The first and most intuitive adaptation of the smashed filter is FFC. For each compressive measurement a single frequency f_u is picked at random and the received signals are linearly combined according to the pseudorandom measurement matrix. Let u_m be a random sampling index with $u_m \in [1, \dots, U]$. In analogy to Eq. (1), FFC can be mathematically expressed as

$$\begin{aligned} \mathbf{y}_m &= \boldsymbol{\phi}_m^T \mathbf{x}_m, \\ \mathbf{x}_m &= (r[u_m, 0], r[u_m, 1], \dots, r[u_m, A-1])^T \end{aligned} \quad (7)$$

where $\boldsymbol{\phi}_m$ is an $A \times 1$ vector. We only consider antipodal patterns, which corresponds to simply inverting some of the received signals before the summing step, as we found them to generally yield better results. Fig. 1 shows the concept of taking one of M compressive measurements using FFC. Note that white elements are zero or simply unconsidered, while grey elements are valued with +1 and black ones with -1.

Clearly, considering only ± 1 as elements of the measurement matrix, which corresponds to a $0^\circ/180^\circ$ phase shift, allows for a simple hardware implementation. Therefore, a single radio frequency frontend would be sufficient, assuming access to a real aperture antenna.

FFC can be further simplified by considering the same frequency for every compressive measurement. Although this leads to the total loss of downrange resolution, it can seriously

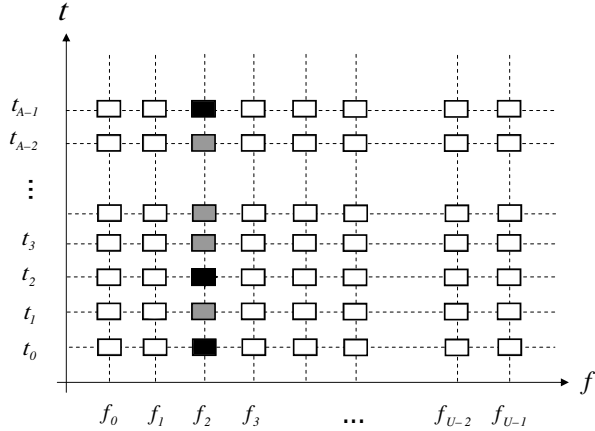


Fig. 1. Fixed Frequency Classification, taking 1 of M compressive measurements

decrease hardware costs since a fixed frequency transceiver setup can be employed.

4.2. Fixed Antenna Element Classification

Considering only one frequency but all antenna elements is not necessarily cost-effective, as additional frequencies are cheap, while additional sensors are usually expensive. Therefore, we introduce FAEC, which randomly chooses an antenna element t_a and linearly combines the values at that element for each frequency to obtain one compressive measurement. Let a_m be a random sampling index with $a_m \in [1, \dots, A]$. In matrix notation, FAEC can be expressed as

$$y_m = \phi_m^T \mathbf{x}_m, \quad (8)$$

$$\mathbf{x}_m = (r[0, a_m], r[1, a_m], \dots, r[U-1, a_m])^T$$

where ϕ_m is an $U \times 1$ vector. Using an antipodal pattern again corresponds to inverting some values before the summing step. The concept of taking one of M compressive measurements using FAEC is depicted in Fig. 2.

FAEC, too, can be further simplified by choosing the same antenna element for every compressive measurement. This allows for a natural and efficient implementation of the smashed filter in real life. If we design a waveform [10] with the appropriate power spectral density to reflect the necessary frequencies, only one pulse has to be transmitted. However, the consideration of only one sensor leads to the total loss of cross-range resolution. In other words, there will be ambiguities between shifted objects, which are located at the same radius from t_a , as they produce the same propagation delay τ_{pa} .

4.3. Template Matching

Template Matching (TM) is the simplest non-compressive alternative to FFC and FAEC, which we will use to assess the

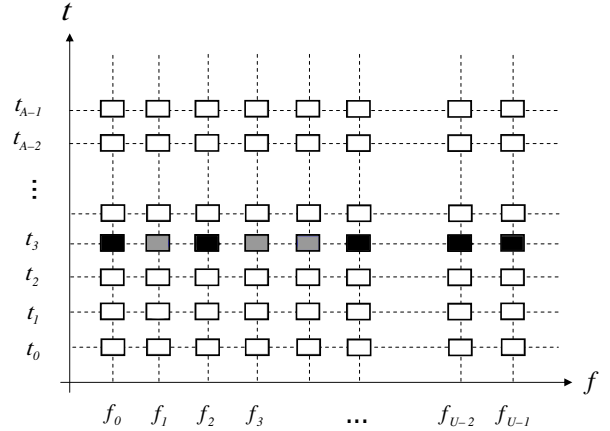


Fig. 2. Fixed Antenna Element Classification, taking 1 of M measurements

performance of these two methods. In this case, the measurement vector \mathbf{y} is simply composed of M non-compressive measurements, which are randomly picked from the original $U \times A$ measurement matrix, which we introduced in Section 3. Subsequently, the smashed filter is applied to \mathbf{y} as previously described.

5. EXPERIMENTAL RESULTS

In the following experiments we evaluate the performance of FFC, FAEC and TM in simulated as well as real TWRI scenarios. To this end, we will estimate the classification rate using a Monte Carlo simulation. Hence, every experiment is executed 1000 times for different values of M and correct classifications are counted. The classification rate, thus, denotes the number of correct classifications in percent. Apart from that, we employ leave-one-out testing, i.e. randomly remove one entry from the training data and use it as the test class in each Monte Carlo run.

For simplicity, we only consider a single class to be present in the observed scene. While the transition to multi-class scenarios is straightforward, the classification process becomes increasingly more complex with each additional class. In order to test every possible combination of classes, we would need to have access to training data for all possible constellations of arbitrarily and individually transformed classes.

5.1. Simulated Data

5.1.1. Simulation Setup

Consider a square target area with a side length of approximately 3.6 m, mapped to a grid of 117×117 pixels. The linear transceiver antenna array consists of $A = 57$ antenna elements—equally spaced at 2.2 cm—and is placed at a distance $z_{\text{off}} = 1.05$ m from the target area. At each element

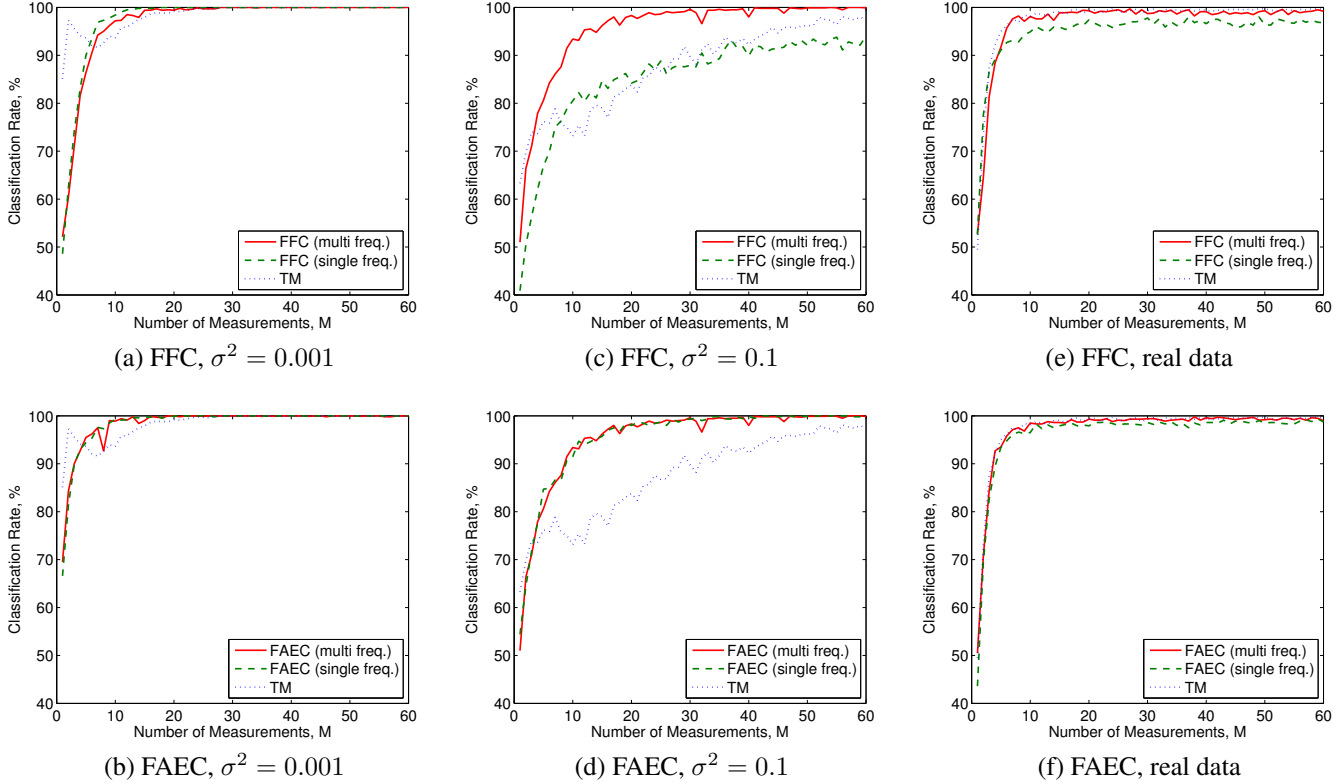


Fig. 3. Classification rates for FFC, FAEC and TM using simulated data under different SNRs (a-d) and real data (e,f)

Class No./No. of targets	Pos. [cross-,downrange] in m
1	[0, 3.5]
2	[-1.25, 3.0] [1.25, 3.0]
3	[-0.75, 2.0] [0, 5.0] [0.75, 2.0]

Table 1. Three point target layouts as simulation classes

position, $U = 801$ measurements are generated, representing multiple frequency steps between 700 MHz and 3.1 GHz.

Table 1 details the point target layouts, which will serve as classes in the following experiments. The training data is generated by successively shifting each point target layout by 1 cm in cross- or downrange. The maximum shift is restricted to 1 m. At this point, we assume free space propagation, i.e. no wall is present.

5.1.2. Results on Simulated Data

A comparison of using FFC, FAEC and TM with different levels of additive noise is given in Fig. 3 (a-d).

Considering a high SNR, i.e. $\sigma^2 = 0.001$, TM leads to a very good classification rate, reaching 100 % for $M \geq 20$, which corresponds to 0.04 % of the available data. FFC and FAEC yield even better results, reaching 100 % already at

about $M = 10$, i.e. using 0.02 % of the data. In the low SNR regime, i.e. $\sigma^2 = 0.1$, the performance of all three algorithms degrades. While TM needs an $M > 70$, i.e. 0.15 % of the data, to achieve perfect classification, FFC and FAEC only require $M \geq 42$ and $M \geq 30$, i.e. 0.09 % and 0.06 % of the data, respectively. If 90% correct classification is sufficient, we can resort to the simplified version of FFC, which uses only one frequency, and thereby decrease hardware costs. All in all, compressive classification outperforms TM in terms of the amount of necessary data, especially in the face of a low SNR.

5.2. Real Data

5.2.1. Experimental Setup

The real measurement setup is similar to the one assumed in the model for simulated data. The 3.6 m \times 3.6 m target scene is set up in an anechoic chamber, the floor of which is not covered by anechoic material. Hence, reflections off the floor will lead to multipath propagation [1]. In contrast to the simulation setup, the transceiving antenna consists of a 57×57 element planar array. Essentially, this gives us 57 complete sets of measurements for different elevation layers. A horn antenna is iteratively moved by 2.2 cm in crossrange and height,

taking measurements for all 801 frequencies at each point. A concrete wall with a thickness of $d = 14.3$ cm and a relative permittivity of $\epsilon = 7.6632$ is placed at a standoff-distance $z_{\text{off}} = 1.05$ m from the antenna. A detailed description of the setup can be found in [1].

We consider TWRI measurements of 4 single objects—a metallic dihedral, a metallic trihedral, a metallic sphere, and a gallon jug of saltwater—placed on a 1.2 m high foam column, located at about 1.9 m downrange. They will serve as classes in the following experiments. For simplicity, we will only consider measurements that were taken using horizontal transmitter and receiver polarization.

5.2.2. Results with Real Data

We do not have access to measurements of shifted objects and, thus, we cannot translate the experiments from the previous section to a real TWRI environment. The 57 available sets of measurements, corresponding to different measurement heights, however, represent some kind of shift, too, only this time the antenna array is shifted instead of the object. Therefore, we will use them as training data for each class.

A comparison of using FFC, FAEC and TM is given in Fig. 3 (e,f). All three methods lead to a similar classification rate, reaching 100 % at about $M = 15$, which corresponds to 0.03 % of the available data. The simplified approaches of FFC and FAEC even yield worse results, as their classification rate saturates slightly below 100 %. Obviously, compressive classification does not offer much benefits in this scenario.

6. CONCLUSION

Two different approaches to modifying the smashed filter for the application in TWRI were presented. They were employed to classify shifted targets in a simulated environment as well as unshifted targets recorded by a shifted antenna in a radar imaging lab. Their performance was evaluated in terms of classification rate and compared to a non-compressive method. While TM already yields excellent results, the compressive methods are able to further reduce the number of measurements. For low SNR, FAEC is the best choice since its performance stays almost constant. FFC and FAEC cannot improve the results of TM in the real data experiment, with all three methods performing equally well.

However, we have to take into account that the two experiments are not perfectly comparable for various reasons. First of all, we consider shifted targets in the simulated case, compared to a shifted antenna in the real setup. Second, the simulation classes are composed of 1 to 3 point targets with the same radar signature, compared to a single target with a different radar signature for each class. Third, the simulated environment lacks a wall and is assumed to be affected by AWGN noise only, while the measurements taken in the radar lab are subject to a huge wall-echo and the noise is not necessarily white. Last, Φ cannot be considered an orthoprojector

in a real radar scenario. Due to the unknown effect of these differences, it is not surprising that the real data results differ from the simulation one.

In order to improve the performance of FFC and FAEC even further, both methods can be extended to consider all four possible combinations of horizontal and vertical transceiver polarizations. That way we can take advantage of the fact that some classes might differ more when viewed from a certain angle.

ACKNOWLEDGEMENT

The authors would like to thank Prof. Dr. Moeness Amin and Dr. Fauzia Ahmad from the Center of Advanced Communications at Villanova University, Villanova, PA, USA, for providing the experimental data.

7. REFERENCES

- [1] F. Ahmad and M. Amin, "Multi-location wideband synthetic aperture imaging for urban sensing applications," *Journal of the Franklin Institute*, vol. 345, pp. 618–639, September 2008.
- [2] E. J. Baranoski, "Through-wall imaging: Historical perspective and future directions," *Journal of the Franklin Institute*, vol. 345, pp. 556–569, January 2008.
- [3] C. Debes, J. Hahn, A. Zoubir, and M. Amin, "Target discrimination and classification in through-the-wall radar imaging," *IEEE Transactions on Signal Processing*, vol. 59, pp. 4664–4676, oct. 2011.
- [4] G. Smith and B. Mobasser, "Robust through-the-wall radar image classification using a target-model alignment procedure," *IEEE Transactions on Image Processing*, vol. 21, pp. 754–767, feb. 2012.
- [5] Y.-S. Yoon and M. Amin, "Compressed sensing technique for high-resolution radar imaging," in *Proceedings of SPIE*, vol. 6968, p. 69681A, 2008.
- [6] M. Leigsnering, C. Debes, and A. M. Zoubir, "Compressive sensing in through-the-wall radar imaging," in *IEEE International Conference on Acoustics, Speech and Signal Processing (ICASSP)*, 2011.
- [7] M. A. Davenport, M. F. Duarte, M. B. Wakin, J. N. Laska, D. Takhar, K. F. Kelly, and R. G. Baraniuk, "The smashed filter for compressive classification and target recognition," *Proc. SPIE Computational Imaging*, vol. 5, January 2007.
- [8] M. F. Duarte, M. A. Davenport, D. Takhar, J. N. Laska, T. Sun, K. F. Kelly, and R. G. Baraniuk, "Single-pixel imaging via compressive sampling," *IEEE Signal Processing Magazine*, vol. 25, pp. 83–91, March 2008.
- [9] G. Alli and D. DiFilippo, "Beamforming for through-the-wall radar imaging," in *Through-the-Wall Radar Imaging* (M. G. Amin, ed.), ch. 3, pp. 81–119, CRC Press, 2011.
- [10] F. Yin, C. Debes, and A. M. Zoubir, "Parametric waveform design for improved target detection," in *European Signal Processing Conference (EUSIPCO)*, August 2011.